

# A diagrammatic formulation of the kinetic theory of fluctuations in equilibrium classical fluids. VI. Binary collision approximations for the memory function for self correlation functions

Joyce E. Noah-Vanhoucke and Hans C. Andersen\*

*Department of Chemistry, Stanford University, Stanford, California 94305*

(Dated: December 1, 2018)

We use computer simulation results for a dense Lennard-Jones fluid for a range of temperatures to test the accuracy of various binary collision approximations for the memory function for density fluctuations in liquids. The approximations tested include the moderate density approximation of the generalized Boltzmann-Enskog memory function (MGBE) of Mazenko and Yip, the binary collision approximation (BCA) and the short time approximation (STA) of Ranganathan and Andersen, and various other approximations derived by us using diagrammatic methods. The tests are of two types. The first is a comparison of the correlation functions predicted by each approximate memory function with the simulation results, especially for the self longitudinal current correlation function (SLCC). The second is a direct comparison of each approximate memory function with a memory function numerically extracted from the correlation function data. The MGBE memory function is accurate at short times but decays to zero too slowly and gives a poor description of the correlation function at intermediate times. The BCA is exact at zero time, but it predicts a correlation function that diverges at long times. The STA gives a reasonable description of the SLCC but does not predict the correct temperature dependence of the negative dip in the function that is associated with caging at low temperatures. None of the other binary collision approximations is a systematic improvement upon the STA. The extracted memory functions have a rapidly decaying short time part, much like the STA, and a much smaller, more slowly decaying part of the type predicted by mode coupling theory. Theories that use mode coupling commonly include a binary collision term in the memory function but do not discuss in detail the nature of that term. It is clear from the present work that the short time part of the memory function has behavior associated with brief binary *repulsive* collisions, such as those described by the STA. Collisions that include attractive as well as repulsive interactions, such as those of the MGBE, have a much longer duration, and theories that include them have memory functions that decay to zero much too slowly to provide a good first approximation for the correlation function. This leads us to speculate that the memory function for density fluctuations can be usefully regarded as a sum of at least three parts: a contribution from repulsive binary collisions (the STA or something similar to it), another short time part that is related to all the other interactions (but whose nature is not understood), and a longer time slowly decaying part that describes caging (of the type predicted by mode coupling theory).

PACS numbers: 05.20.Dd, 05.20.Jj, 61.20.-p

## I. INTRODUCTION

The concept of uncorrelated binary collisions<sup>1</sup> has played an important role in the development of the kinetic theory of fluids.<sup>2</sup> It is a central idea in the Boltzmann kinetic equation for dilute gases, the Enskog equation for high density liquids, and generalizations of Enskog theory that take into account the softness of the repulsive potential.<sup>3,4,5,6,7</sup> The nature of the binary collisions in the Boltzmann and Enskog theories are very different, involving in one case the entire interparticle potential, and in the other case only the repulsive part of the potential, which is idealized as a hard sphere potential.

For kinetic theories of dense liquids that do take into account the effect of both the attractive and repulsive parts of the interatomic potential on the dynamics, the different range, strength, and effects of the two parts of the potential has motivated the construction of theories that treat these two parts very differently. Examples include the Rice-Allnatt theory<sup>8,9,10</sup> and the Karkheck-

Stell theory.<sup>11,12,13,14,15,16,17</sup>

The equilibrium theory of the structure and thermodynamics of liquids shows similar developments. At low density, both the radial distribution function and the thermodynamic properties are represented by relatively simple expressions that contain the entire potential. At higher density, various theories have invoked the primacy of the repulsive forces for determining the structure.<sup>18,19,20,21,22,23,24</sup> Theories that take into account both types of forces at high density often calculate the effect of attractions using very different ideas from those used for repulsive forces.<sup>18,21,22,25,26</sup>

Theories of equilibrium structure and thermodynamics have been derived and formulated in a variety of ways, including perturbation theory, integral equations, and cluster expansions.<sup>27,28</sup> The Mayer cluster theory and its extensions<sup>28,29,30,31</sup> provide a unifying theoretical framework for deriving and analyzing many of these theories (and many others) and relating them to one another. The Mayer theory represents the static correlation functions and free energy of a fluid in terms of an infinite

set of diagrams. Approximations are typically developed by identifying certain subsets of diagrams, summing them, and discarding the others. A standard tactic in cluster theory is to decompose the objects in the theory that represent interactions into various pieces and include the various pieces in different ways in developing approximations.<sup>23,24,30,31</sup>

A focus on interparticle forces and their effects on dynamics is quite different from the perspective provided by the fully renormalized kinetic theory of Mazenko and co-workers.<sup>32,33,34,35,36</sup> In the latter approach, the theory of the correlation functions for density fluctuations in equilibrium liquids is formulated in such a way that the interparticle potential does not appear; instead, only the equilibrium static correlation functions, such as the pair correlation function and its generalization to more than two particles, appear in the final results. In effect, the dynamics is expressed in terms of the potentials of mean force rather than the ‘bare’ potential.

One of the results of this theory was a generalized Boltzmann-Enskog memory function (denoted GBE) for fluids and an approximation to this function that they called the ‘moderate density approximation’ to the generalized Boltzmann-Enskog memory function (denoted MGBE). The latter can be interpreted physically as taking into account uncorrelated binary collisions among the particles, with the potential that determines the dynamics being the potential of mean force rather than the bare potential.

In recent work, Young and Andersen<sup>37,38</sup> used molecular dynamics simulations to study the behavior of several pairs of atomic liquids. Each pair consisted of two systems at the same density but different temperatures, with very similar pair correlation functions, and hence very similar potentials of mean force, despite their very different interparticle potentials. It was found that some (but not all) of the features of the dynamics of such a pair of liquids were very similar, suggesting that the potential of mean force is in some sense a more important determinant of dynamics than is the bare potential itself. This is consistent with the basic ideas of renormalized kinetic theory.

A formally exact diagrammatic formulation of the kinetic theory of density correlation functions was developed by one of us.<sup>39,40,41</sup> It expresses the dynamic correlation functions of the particle density in terms of an infinite series of diagrams in a way analogous to the infinite series in the Mayer cluster theory for equilibrium static correlation functions. The vertices of the graphs, which represent interactions among particles, are expressed in terms of static correlation functions, and the theory is fully renormalized in the sense of Mazenko. This theory can provide a unifying theoretical framework for deriving and analyzing kinetic theories of density fluctuations in liquids.

Using this graphical theory, Ranganathan and Andersen<sup>42,43</sup> considered the case of a fluid whose interatomic potential contained a continuous but very re-

pulsive short ranged part, as well as longer ranged attractions. Using the inverse of the strength of the short ranged force as a small parameter, they determined the diagrams that are most important for the short time behavior of the memory functions for the dynamic correlation function for density fluctuations. This analysis involved a procedure much like the one discussed above for the Mayer theory, namely a decomposition of the fully renormalized quantities that appear in the diagrams of the theory into various contributions with different characteristics in the limit as the small parameter goes to zero. The most important diagrams (*i.e.* the most divergent diagrams) were identified. Summing this infinite series of diagrams exactly led to an approximation for the memory function that is called the short time approximation (STA). The structure of this approximation indicates that it takes into account uncorrelated binary collisions involving the repulsive part of the potential, with a collision frequency that is determined by the structure of the fluid (and hence is influenced by the attractive forces).

Using this short time approximation and neglecting the longer time contributions to the memory function gives a kinetic theory that can be regarded as a generalization of the Enskog theory to dense fluids with continuous repulsive forces as well as attractive forces. The Enskog kinetic equation is local in time, with no memory of the past history. As a result, the memory function in the Enskog theory is proportional to a Dirac delta function in time. For fluids with continuous repulsive potentials, there is a part of the memory function that is very large at very short times<sup>44</sup> and that approaches a delta function in time as the repulsive part of the potential approaches a hard sphere potential. The STA includes all diagrammatic contributions to that large, short-lived part of the memory function. This is the sense in which the STA is a generalization of the Enskog theory.

The predictions of this theory have been tested by comparison with computer simulation studies of the Lennard-Jones fluid.<sup>43</sup> The accuracy of the theory is different for different correlation functions but is surprisingly good at high temperatures for the viscosity and diffusion constant. The theory fails to describe the changes in correlation functions that take place as a dense high temperature fluid is cooled to the triple point temperature. In particular, the increasingly negative dip in the velocity autocorrelation function and the self-longitudinal current are not well described, suggesting that the dynamics in the vicinity of the triple point requires much more than uncorrelated repulsive binary collisions for its description.

Ranganathan and Andersen also identified a more general set of diagrams whose sum leads to an approximation, called the binary collision approximation (BCA), that describes the effect of uncorrelated binary collisions that are determined by the potential of mean force. (The relationship of this to the moderate density approximation of the generalized Boltzmann-Enskog memory function will be discussed in more detail below.)

In this paper, we discuss a variety of ways in which binary collisions might be defined for use in approximations based on uncorrelated binary collisions. We test several of them by comparing their predictions with the results of molecular dynamics simulations of a dense Lennard-Jones liquid at various temperatures, from the triple point temperature to four times that value. There were several motivations for this work.

1. There are many different possibilities for specifying the nature of the binary collisions in dense fluids. Some of them are mentioned above. Others are suggested by the possibility of breaking the potential of mean force, which appears in fully renormalized kinetic theory, into various contributions and describing the effect of the various contributions in different ways, in analogy to the way in which the bare potential is decomposed in both kinetic theory and the equilibrium theory of fluids. Moreover, the diagrammatic kinetic theory suggests some straightforward extensions of binary collision approximations (as is discussed below).

2. It would be worthwhile to test the various approximations by direct comparison of their predictions with computer simulation studies in order to determine which of them provides, in some sense, the best starting point for further development of kinetic theory.

3. The mode coupling theory of Götze and coworkers, and the kinetic theory that provides the basis for it,<sup>45,46,47</sup> focusses on the long time behavior of the memory function for density correlations in a fluid, but it assumes that there is a short time part that represents brief and presumably binary collisions between the atoms. However, the theory does not provide a microscopic expression for this short time part, and in practice its contribution is described by a simple empirical function of time obtained by fitting to simulation or experimental data. It would be worthwhile to understand the nature of the true short time behavior of the memory function as a starting point for understanding the approximations made in mode coupling theory and attempting to go beyond those approximations.

Our discussion will rely heavily on the diagrammatic kinetic theory<sup>39,40,41,42</sup> as a unifying framework for stating and comparing the various approximations as well as for deriving some of them. We restrict attention to dense atomic liquids (rather than gasses) with short range forces (rather than Coulombic forces). We also restrict attention to theories that calculate and use a memory function to calculate the equilibrium time correlation functions of the density in phase space. Finally, the correlation functions we focus on in this paper are self (or incoherent) correlation functions.

## II. BINARY COLLISION APPROXIMATIONS AND THE DIAGRAMMATIC THEORY

### A. Self correlation function

We are concerned with the kinetic theory of the self correlation function of density fluctuations in a dense atomic fluid. The incoherent scattering function and self-diffusion are experimental observables associated with this function. (For additional studies that deal with other correlation functions, see Ref. 48.)

The system of interest is a single component classical atomic fluid at equilibrium. Its Hamiltonian is

$$H(\mathbf{r}^N, \mathbf{p}^N) = \sum_{i=1}^N |\mathbf{p}_i|^2 / 2m + \sum_{i < j=1}^N u(|\mathbf{r}_i - \mathbf{r}_j|)$$

The self part of the two-point time correlation function for density fluctuations in single particle phase space is

$$C^{(s)}(11', t) \equiv \frac{1}{\rho} \left\langle \sum_{i=1}^N \delta f_i(1, t) \delta f_i(1', 0) \right\rangle$$

where  $\rho = N/V$  is the number density,

$$f_i(1, t) = \delta(\mathbf{R}_1 - \mathbf{r}_i(t)) \delta(\mathbf{P}_1 - \mathbf{P}_i(t))$$

is the density in single particle phase space for particle  $i$ , and

$$\delta f_i(1, t) \equiv f_i(1; t) - \langle f_i(1; t) \rangle$$

is a density fluctuation. We use numbers like 1, 2, *etc.* to represent points in single particle phase space, *e.g.*,  $1 = \mathbf{R}_1 \mathbf{P}_1$ ,  $2' = \mathbf{R}_{2'} \mathbf{P}_{2'}$ . Angular brackets denote equilibrium ensemble averages.

The kinetic equation for this correlation function is

$$\begin{aligned} \frac{\partial}{\partial t} C^{(s)}(11', t) \\ = \int_0^t dt' \int d3 M^{(s)}(13; t-t') C^{(s)}(31', t') \end{aligned} \quad (1)$$

where the self part of the memory function  $M^{(s)}$  is the sum of two terms

$$M^{(s)}(11', t) = M_f(11', t) + M_c^{(s)}(11', t)$$

The flow term is

$$M_f(11', t) = -\frac{\mathbf{P}_1}{m} \cdot \nabla_{\mathbf{R}} \delta(11') \delta(t)$$

We use the notation  $\delta(11') = \delta(\mathbf{R}_1 - \mathbf{R}_{1'}) \delta(\mathbf{P}_1 - \mathbf{P}_{1'})$  and  $\nabla_{\mathbf{R}} \delta(11')$  is the gradient of  $\delta(11')$  with respect to the first position argument. We make approximations for  $M_c^{(s)}$ , the collisional part of the self memory function, which we shall simply refer to as the memory function.

The initial condition for eq. (1) is

$$C^{(s)}(11', 0) = \rho M_m(1) \delta(11')$$

where  $M_m$  is the Maxwell-Boltzmann distribution of momenta

$$M_m(1) \equiv (2\pi m k_B T)^{-3/2} \exp(-|\mathbf{P}_1|^2 / 2m k_B T)$$

and  $g(11') \equiv g(|\mathbf{R}_1 - \mathbf{R}_{1'}|)$  is the pair correlation function of the fluid.

## B. Diagrammatic series

The diagrammatic kinetic theory provides several closely related expressions for the correlation function  $C^{(s)}$  and the memory function  $M^{(s)}$  as the sum of the values of an infinite series of diagrams of a certain topological structure.<sup>39,40,42</sup> The diagrams contain propagators that describe the time evolution of density fluctuations and vertices that represent renormalized interactions among those fluctuations. We shall focus on the two formulations of these series that are most useful for the present discussion.

The first form of diagrammatic series<sup>40</sup> contains  $\chi^{(0)}$  propagators, which describe density fluctuations at sets of one or more points in the fluid, and  $Q$  vertices.

The second form of the diagrammatic series<sup>49</sup> contains  $\chi^{(fp)}$  propagators, each of which describes the propagation of a single density fluctuation associated with a single particle that moves according to free particle motion, and  $Q^{(c,p)}$  vertices, which describe the localized interactions among such density fluctuations.

The two series are each formally exact. The second is derived from first. The first is useful for proving some formal properties of the series, such as symmetry properties. In practice, the second is more useful for deriving practical approximations. In the second series it is possible to identify density fluctuations in different parts of a diagram and interpret them as being caused by the presence (or absence) of the same particle. The vertices in the theory are calculated from static correlation functions of the fluid, and so it is possible to identify how many distinct correlated particles are associated with a vertex. The identification of the number of particles associated with a vertex is in some cases ambiguous, for reasons that we will discuss, but it is still possible to identify terms that correspond to, for example, the interaction of two particles, and hence it is possible to discuss whether diagrams describe binary collisions.

Additional diagrammatic series can be derived from the second series by expressing the vertices as sums of various contributions. For example, in vertices that contain the potential of mean force, the latter can be decomposed into a short ranged repulsive part and a longer ranged oscillatory part, leading to the original vertex being expressed as a sum of two new vertices. The resulting

diagrammatic series can then be used to develop approximations in which the effects of the two parts of the potential are taken into account in different ways. (When an approximation is made to a diagrammatic series for a correlation function, by neglecting some diagrams and/or approximating certain vertices, the resulting approximation may or may not be consistent with known symmetry properties of the correlation function, such as stationarity and time reversal symmetry. See Appendix A for a discussion.)

## C. Diagrammatic characterization of various approximations

### a. Generalized Boltzmann-Enskog memory function.

This memory function, denoted GBE, is generated in Mazenko's theory by neglecting a function  $\Gamma$ , which represents renormalized dynamical interactions, in the equation of motion for a function in terms of which the memory function of interest is expressed.<sup>50</sup> In terms of the first diagrammatic series, it represents the sum of all diagrams in the series for the memory function in which there are at most two density fluctuations propagating at any time.

This approximation satisfies important symmetry properties exactly (see Appendix A). Moreover, it gives exactly the correct value of the memory function at  $t = 0$ . However, it is not clear how it might be calculated in any practical fashion, and to our knowledge numerical calculations of the GBE memory function have never been performed. The physical meaning of the approximation is hard to specify but the mathematical meaning in the context of the diagrammatic theory is clear. It contains contributions to the memory function that describe two density fluctuations that interact with each other and propagate. The identities of the two particles associated with the two fluctuations can be different at different times. All interactions and propagations of the two fluctuations are treated exactly. The approximation that is made is to neglect the possibility of three or more simultaneous fluctuations.

b. *Binary collision approximation.* This approximation, denoted BCA, was defined in Ref. 42 in terms of the second diagrammatic series. It is the sum of all diagrams in the series for the GBE memory function in which the same pair of particles is associated with the fluctuations at all times.

This approximation does not satisfy important symmetry properties exactly (see Appendix A). However, it does give exactly the correct value for  $M^{(s)}$  at  $t = 0$ . A practical algorithm exists to evaluate it, as is discussed below.

The physical meaning of the approximation is that it contains contributions to the memory function that describe two density fluctuations, associated with two specific particles, that interact with each other and propagate, without having three fluctuations present at any

time. All interactions and propagations of the two fluctuations are treated exactly. The approximation here is not only to neglect the possibility of three or more simultaneous fluctuations (as in the GBE) but also to neglect diagrams in which the two fluctuations at one time represent a different pair of particles than the two fluctuations at other times. This characterization is the reason why it can be regarded as a binary collision approximation, *i.e.* one that involves only two particles.

*c. The moderate density approximation to the generalized Boltzmann-Enskog memory function.* This memory function, denoted MGBE, was defined by Mazenko as an approximation to the GBE. Various quantities in the GBE are defined in terms of static correlation functions of the fluid. To construct the MGBE, the contributions to these quantities that contain three and four particle correlation functions are deleted.<sup>51</sup>

The deletion of the three and four particle correlation functions to define the MGBE is closely related to, but not equivalent to, what is done in defining the BCA to include diagrams in which fluctuations representing at most two distinct particles appear. (See Appendix B.) The MGBE is almost equivalent to the BCA, except for one factor in every diagram. From a diagrammatic point of view, the MGBE can be regarded as an approximation to the BCA in which the vertex  $Q_{12}$  that appears in each diagram is replaced by an approximation that contains the potential of mean force. (A detailed expression for the MGBE is given below, together with a comparison to the BCA.)

This approximation satisfies important symmetry properties exactly (see Appendix A). It does not give exactly the correct value of the memory function at  $t = 0$ . A practical algorithm exists to evaluate it, as is discussed below.

The physical meaning of the MGBE is equivalent to that of the BCA. The only difference is that the additional approximation made to the  $Q_{12}$  leads to a binary collision approximation that satisfies the symmetry condition.

*d. Short time approximation.* This will be referred to as the STA. This was derived<sup>42</sup> from the second diagrammatic series using the procedure discussed above, namely expansion of the diagrams in powers of a small parameter representing the inverse of the strength of the repulsive part of the potential and retaining those terms that at short times are most divergent. The diagrams that appear are those of the BCA, as defined above, but with vertices that contain the repulsive part of the interatomic potential, rather than the potential or the potential of mean force. (See below for a more precise statement of the value of the STA.)

The STA satisfies the symmetry property approximately, but not exactly. (In the limit of infinitely repulsive forces, it satisfies the symmetry property exactly. See Appendix A.) It does not give exactly the correct value of the memory function at  $t = 0$ . A practical algorithm exists to evaluate it.

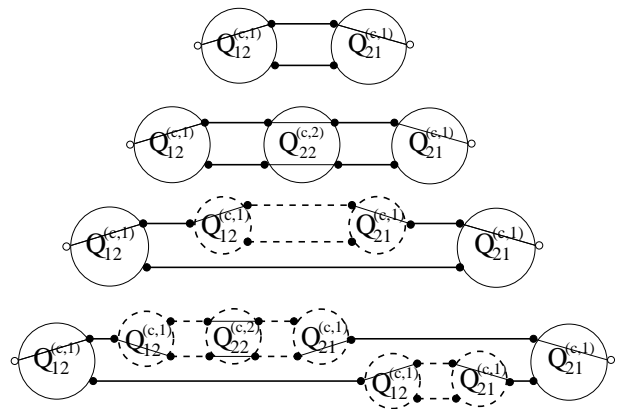


FIG. 1: The first two diagrams are members of the diagrammatic series for the binary collision memory functions. (The remaining diagrams in the binary collision memory functions have additional  $Q_{22}^{(c,2)}$  vertices on the two horizontal particle paths.) The third and fourth diagrams are examples of diagrams that are not in a binary collision memory function. One or both of the two particles is interacting separately with a third particle in an STA approximation. The parts of the diagrams that have these STA interactions are indicated with dashed lines and dashed circles. (See the text and Fig. 2 for additional discussion.)

*e. Other binary collision approximations.* Below we shall discuss several approximations whose diagrammatic meaning is straightforward. Like the STA, they can be defined graphically by starting with the BCA, separating each of the vertices into two terms, and retaining only the first term. The physical meaning of such an approximation depends on the nature of the separation. The reason for investigating such approximations is the desire to develop better binary collision approximations as a starting point for a more general kinetic theory.

*f. Beyond the binary collision approximation.* A major restrictive assumption of all the approximations mentioned above is that the possibility of having three or more simultaneous density fluctuations is ignored. The pair of particles that are associated with the two density fluctuations interact with each other, but the presence of other particles is taken into account only in some average sense, if at all, due to the appearance of static pair correlation functions of the fluid in the various vertices.

It is relatively simple, in the context of a graphical theory, to construct approximations that relax these assumptions in a physically meaningful way. The first two diagrams in a binary collision approximation are shown as the first two diagrams in Fig. 1. The generic BCA diagram consists of two particle paths<sup>42</sup> that propagate from the  $Q_{21}^{(c,1)}$  vertex on the right to the  $Q_{12}^{(c,1)}$  vertex on the left. In between these vertices are zero or more  $Q_{22}^{(c,2)}$  vertices. These diagrams describe the propagation of a pair of particles that interact with each other using the potential that is contained within the  $Q_{22}^{(c,2)}$  function. To develop the  $K$  approximations, consider including di-

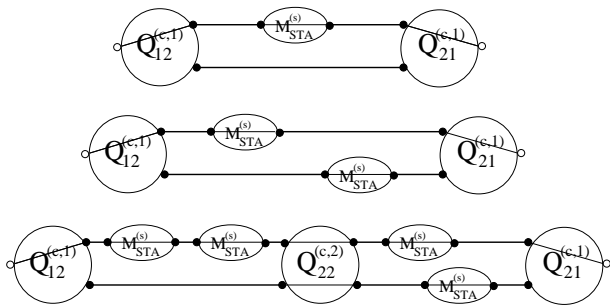


FIG. 2: Examples of diagrams in a binary collision approximation augmented with  $M_{STA}^{(s)}$  memory functions on the particle paths to represent interactions with third particles of the type shown in Fig. 1. The first diagram here includes the third diagram of Fig. 1. The second diagram here includes the fourth diagram of Fig. 1. The generic member of this series is obtained by taking the generic member of the series for a binary collision approximation (see the first two diagrams in Fig. 1 for examples) and inserting an arbitrary number of  $M_{STA}^{(s)}$  memory functions on each of the lines. (See the text and Fig. 1 for additional discussion.)

agrams in the exact graphical series that are similar to these and that are constructed by inserting STA memory functions into the propagators on the particle paths of the original diagrams of the BCA. The diagrams that result are those of the original BCA diagrams with any number of STA memory functions inserted. See Fig. 2.

When the diagrams with STA memory functions are evaluated, the two points have different times associated with them and the STA memory function is a function of the time difference. Since the collisions are brief, we approximate the effect of these vertices using a BGK model.<sup>52</sup> The BGK model memory function is

$$M_K(11'; t) = \nu m_K(11') \delta(t)$$

where  $m_K(11') = -\delta(\mathbf{P}_1 - \mathbf{P}'_1) + M_m(\mathbf{P}_1)$  and  $\nu$  is a collision frequency. The BGK model is an approximate memory function that is instantaneous in time. It approximates a collision as having the effect of replacing the momentum of the particle by a new random momentum drawn from a Maxwell-Boltzmann distribution. Because of its simplicity, its effect can easily be incorporated into the algorithm for evaluating binary collision approximations, as is discussed below.

This procedure allows any binary collision approximation to be converted into one that also includes brief uncorrelated binary collisions of each of the two particles with third particles or fluctuations in the surrounding fluid. Graphically this is done by inserting  $M_K$  vertices, as approximations for STA memory functions, into the  $\chi^{(fp)}$  propagators that by themselves describe free particle propagation. When this procedure is applied to any approximation, the resulting approximation will be given a name with “K” as a prefix. Thus, for example, the MGBE approximation, when modified in this way, will be called the K-MGBE approximation. In constructing

such an approximation, the value of the parameter  $\nu$  must be chosen. This will be discussed below.

We shall refer to this class of approximations as  $K$  approximations.  $K$  approximations are mathematically and physically similar to a type of approximation suggested by Mazenko and Yip.<sup>53</sup>

#### D. Analytic formula for the BCA and related approximations

The various approximations mentioned above, with the exception of the GBE approximation, can be expressed in terms of very similar analytic formulas for  $M^{(s)}$ . As a result, all of them can be evaluated with a similar algorithm. Here we will state the formulas. The algorithm will be discussed later.

For the BCA, the memory function is

$$M_{BCA}^{(s)}(1t, 1't') = \int d2 d3 d4 d5 \quad (2)$$

$$\times Q_{12}^{(c,1)}(1; 23) \chi_{BCA}(23t; 45t') Q_{21}^{(c,1)}(45; 1')$$

where the  $Q$  vertices represent interaction terms and the  $\chi_{BCA}$  term is a response function. The detailed equations for these functions are

$$Q_{12}^{(c,1)}(1; 1'2') = \nabla_{\mathbf{R}} V_{12}(12') \cdot \nabla_{\mathbf{P}} \delta(11') \quad (3)$$

$$Q_{21}^{(c,1)}(12; 1') \quad (4)$$

$$= \frac{M_m(1)}{M_m(1')} \rho(2) M_m(2) g(12) \nabla_{\mathbf{R}} V_{21}(12) \cdot \nabla_{\mathbf{P}} \delta(11')$$

$$\chi_{BCA}(12t; 1'2't') \quad (5)$$

$$= e^{-i\mathcal{L}(12)(t-t')} \delta(11') \delta(22') \Theta(t-t')$$

The Liouville operator  $\mathcal{L}$  is

$$\mathcal{L}(12) = L_0(1) + L_0(2) + \tilde{L}_1(12) \quad (6)$$

$$L_0(1) = -i \frac{\mathbf{P}_1}{m(1)} \cdot \nabla_{\mathbf{R}_1} \quad (7)$$

$$\tilde{L}_1(12) = i \nabla_{\mathbf{R}} V_{22}(12) \cdot (\nabla_{\mathbf{P}_1} - \nabla_{\mathbf{P}_2}) \quad (8)$$

These formulas contain three functions  $V_{12}$ ,  $V_{21}$  and  $V_{22}$  that are two particle potentials. For the BCA, they are

$$V_{12}(12) = u(12); \quad V_{21}(12) = V_{22}(12) = v_{MF}(12) \quad (9)$$

where  $u(12)$  is the interparticle potential and  $v_{MF}(12) = -k_B T \ln g(12)$  is the potential of mean force, and  $g(12)$  is the pair correlation function.

The BCA is exact in the low density limit and corresponds to the linearized Boltzmann equation in that limit on appropriate length and time scales. The  $\chi_{BCA}$  describes two particle scattering with an effective interparticle potential that is the potential of mean force, which also appears in  $Q_{21}$ . At low density, the potential of mean force approaches the bare potential. The BCA describes binary collisions (on microscopic length and time

Approximation	$V_{12}$	$V_{21}$	$V_{22}$	$\hat{M}_{\hat{k}\hat{k}}(\mathbf{k}, 0)$
STA	$u_r(r)$	$u_r(r)$	$u_r(r)$	-332
BCA	$u(r)$	$v_{MF}(r)$	$v_{MF}(r)$	-281
K-BCA	$u(r)$	$v_{MF}(r)$	$v_{MF}(r)$	-281
MGBE	$v_{MF}(r)$	$v_{MF}(r)$	$v_{MF}(r)$	-289
K-MGBE	$v_{MF}(r)$	$v_{MF}(r)$	$v_{MF}(r)$	-289
RPMF	$v_{rMF}(r)$	$v_{rMF}(r)$	$v_{rMF}(r)$	-215
K-RPMF	$v_{rMF}(r)$	$v_{rMF}(r)$	$v_{rMF}(r)$	-215
hybrid				
MGBE/STA	$v_{MF}(r)$	$v_{MF}(r)$	$u_r(r)$	-289

TABLE I: A table of all approximations studied, stating the necessary potential functions that define a binary collision approximation for the memory function and the value of the  $\hat{k}\hat{k}$  matrix element of the memory function at  $t = 0$ . The BCA value for  $\hat{M}_{\hat{\mu}\hat{\nu}}(\mathbf{k}, 0)$  is exact. Note that  $u(r)$  is the bare potential,  $u_r(r)$  is the repulsive part of the bare potential,  $v_{MF}(r)$  is the potential of mean force, and  $v_{rMF}(r)$  is the repulsive part of the potential of mean force. Details about approximations not discussed in this text can be found in Ref. 48.

scales) in much the same way as the Boltzmann equation, with some many body effects accounted for in the effective potential.

The MGBE is of the same form as eqs. (2)–(8), with (9) replaced by

$$V_{12}(12) = V_{21}(12) = V_{22}(12) = v_{MF}(12) \quad (10)$$

The STA is of the same form as eqs. (2)–(8), with (9) replaced by

$$V_{12}(12) = V_{21}(12) = V_{22}(12) = u_r(12)$$

where  $u_r(12)$  is the repulsive part of the potential  $u(12)$ .

Any other binary collision approximation, as discussed above, leads to results of the form of eqs. (2)–(8), with the potentials  $V_{12}$ ,  $V_{21}$ , and  $V_{22}$  being the functions used in the approximation. See Table I for a list of various approximations we have considered.

Any  $K$  approximation, as discussed above, leads to results of the form of eqs. (2)–(8) with eq. (6) replaced by

$$\begin{aligned} \mathcal{L}_K(12) & \quad (11) \\ & = L_0(1) + L_0(2) + \tilde{L}_1(12) + \tilde{L}_{BGK}(1) + \tilde{L}_{BGK}(2) \end{aligned}$$

The symmetry properties of the various approximations are discussed in Appendix A.

### III. CALCULATIONS

#### A. Basis function expansion of the kinetic equation

Using the expressions for the  $Q$  vertices and  $\chi_{BCA}$  response function, the expression in eq. (2) leads to

$$\begin{aligned} M_{BCA}^{(s)}(1t; 1't') & = \int d2 d3 d4 d5 \frac{M_m(4)}{M_m(1')} \rho(5) M_m(5) g(45) \\ & \times (\nabla_{\mathbf{R}} V_{12}(13) \cdot \nabla_{\mathbf{P}} \delta(12)) \cdot (\nabla_{\mathbf{R}} V_{21}(45) \cdot \nabla_{\mathbf{P}} \delta(41')) \\ & \times e^{i\mathcal{L}(23)(t-t')} \delta(24) \delta(35) \Theta(t-t') \end{aligned}$$

It is convenient to take the Fourier transform of  $C^{(s)}$  and  $M^{(s)}$  with regard to the difference in their position arguments and to represent their momentum dependence in terms of a set of Hermite polynomial basis functions. The details of the Hermite polynomial expansion are discussed in Ref. 48. From eq. (2), we can obtain the following expression for the Fourier transformed matrix elements of  $M^{(s)}$

$$\begin{aligned} \hat{M}_{\hat{\mu}\hat{\nu},BCA}^{(s)}(\mathbf{k}, t) & = - \int d\mathbf{P}_1 d\mathbf{R}_2 d\mathbf{P}_2 g(|\mathbf{R}_1 - \mathbf{R}_2|) \\ & \times M_m(\mathbf{P}_1) \rho M_m(\mathbf{P}_2) (\nabla V_{Q_{21}}(|\mathbf{R}_1 - \mathbf{R}_2|) \cdot \nabla h_{\vec{\nu}}(\mathbf{P}_1)) \\ & \times e^{-i\mathbf{k} \cdot \mathbf{R}_a} (\nabla V_{Q_{12}}(|\mathbf{R}_a - \mathbf{R}_b|) \cdot \nabla h_{\vec{\mu}}(\mathbf{P}_a)) \quad (12) \end{aligned}$$

The  $\vec{\mu}$  and  $\vec{\nu}$  are labels for the Hermite polynomial basis functions. Each is an ordered triplet of nonnegative integers. (In the following, we shall use ‘ $\vec{0}$ ’ as an abbreviation for the triplet ‘000’ and ‘ $\hat{k}$ ’ as an abbreviation for ‘001’.) Note that  $M_{\hat{\mu}\hat{\nu}}^{(s)} = 0$  if either  $\vec{\mu} = 0$  or  $\vec{\nu} = 0$ .  $M_{\hat{k}\hat{k}}^{(s)}$  is the single most important matrix element of the memory function. In the limit of small wave vector and/or short time, it is the only matrix element that contributes to the correlation function, and in general it is the matrix element that most strongly affects the time dependence of the correlation function.) In eq. (12),  $\mathbf{R}_1$  is defined to be the origin and the phase points  $\mathbf{R}_1 \mathbf{P}_1 \mathbf{R}_2 \mathbf{P}_2$  are the initial conditions for two particles that evolve forward in time according to Hamilton’s equations of motion with  $V_{22}$  as the interatomic potential to the final phase points  $\mathbf{R}_a \mathbf{P}_a \mathbf{R}_b \mathbf{P}_b$  at time  $t$ . The matrix elements of the memory function are calculated using the two particle trajectory calculation method of Ranganathan and Andersen.<sup>43</sup> See Appendix C for details and for a discussion of the error analysis.

The correlation functions of interest in this work are the self correlation functions: the incoherent intermediate scattering function (IISF)

$$\hat{F}_s(\mathbf{k}, t) = \hat{C}_{\vec{0}\vec{0}}^{(s)}(\mathbf{k}, t) = \frac{1}{N} \left\langle \sum_{i=1}^N e^{-i\mathbf{k} \cdot (\mathbf{r}_i(t) - \mathbf{r}_i(0))} \right\rangle$$

and the self longitudinal current correlation function

(SLCC)

$$\begin{aligned} \hat{J}_{ls}(k, t) &= \hat{C}_{\hat{k}\hat{k}}^{(s)}(k_z, t) \\ &= \frac{1}{N} \left\langle \sum_{i=1}^N \frac{p_{iz}(t)}{m} \frac{p_{iz}(0)}{m} e^{-ik_z(r_{iz}(t) - r_{iz}(0))} \right\rangle \end{aligned}$$

In these equations it is to be understood that the wave vector  $\mathbf{k}$  is in the  $z$ -direction. The IISF and SLCC functions are related in the following way

$$\hat{J}_{ls}(\mathbf{k}, t) = -\frac{1}{|\mathbf{k}|^2} \frac{\partial^2}{\partial t^2} \hat{F}_s(\mathbf{k}, t)$$

In the graphs below, the SLCC is normalized so that its value at unity is  $t = 0$ . We focus on the SLCC because we have found its qualitative features to be sensitive to errors in binary collision approximations. For a discussion of additional correlation functions, see Ref. 48.

For some of the discussion we will need two related functions. The first is the total correlation function

$$C(11', t) = \langle \delta f(1, t) \delta f(1', 0) \rangle$$

where

$$f(1, t) = \sum_{i=1}^N \delta(\mathbf{R}_1 - \mathbf{r}_i(t)) \delta(\mathbf{P}_1 - \mathbf{p}_i(t))$$

is the total particle density and

$$\delta f(1, t) \equiv f(1, t) - \langle f(1, t) \rangle$$

is a density fluctuation. The second function is the Fourier transform of  $C(11', t)$ , the coherent intermediate scattering function (ISF)

$$\hat{F}(\mathbf{k}, t) = \hat{C}_{\hat{0}\hat{0}}(\mathbf{k}, t) = \frac{1}{N} \left\langle \sum_{i,j=1}^N e^{-i\mathbf{k} \cdot (\mathbf{r}_i(t) - \mathbf{r}_j(0))} \right\rangle$$

## B. Solution of the kinetic equations

Use of the Hermite polynomial basis set for the momentum arguments converts the kinetic equation for  $\hat{C}^{(s)}(\mathbf{k}, t)$  into an infinite dimensional matrix equation for the matrix elements of  $\hat{C}^{(s)}$ . We solve this infinite dimensional equation numerically using the method of Ranganathan and Andersen.<sup>43</sup> In this method, the equations for successively larger finite sets of coupled equations are solved. Each of these finite sets is chosen such that its solution agrees with the exact solution of the infinite set up to order  $t^n$  for small  $t$ , and successive finite sets have increasing values of  $n$ . When the successive solutions no longer change with increasing  $n$ , the last result is regarded as the solution to the infinite set. A detailed discussion of the method can be found in Ref. 54.

The IISF, which corresponds to  $\hat{C}_{\hat{0}\hat{0}}^{(s)}(\mathbf{k}, t)$ , is converged with the  $\mathcal{O}(t^9)$  approximation. The SLCC, which corresponds to  $\hat{C}_{\hat{k}\hat{k}}^{(s)}(\mathbf{k}, t)$ , is converged with the  $\mathcal{O}(t^7)$  approximation. We present only these solutions in the results that follow. Moreover, we concentrate on the results for the SLCC since none of the approximations are able to consistently reproduce all of the features of this function, especially the temperature dependence of the negative region for the function. Since the SLCC is proportional the second derivative of the IISF, the accuracy of an approximation for the SLCC function is consistent with its accuracy for the IISF.

## C. Molecular dynamics calculations

The correlation functions calculated from the binary collision approximations for the memory function will be compared to results generated from molecular dynamics simulations of a 500-particle, one component Lennard-Jones liquid at equilibrium.<sup>37,38,55</sup> The states of interest are reduced density  $\rho = 0.85$  (approximately the triple point density) at reduced temperatures  $T = 0.723, 1.554, 3.000$  (the triple point temperature is approximately 0.723). Results for temperatures between 0.723 and 1.554 at  $\rho = 0.85$ , and high temperature results at  $\rho = 0.75$  can be found in Ref. 48. The usual reduced units for the Lennard-Jones fluid are used.<sup>56</sup> The correlation function results from molecular dynamics simulation and the binary collision approximations have small statistical error whose values are generally smaller than the differences between the simulation data and the theoretical curves. The details of the molecular dynamics simulations can be found in Refs. 37 and 38.

## IV. RESULTS

### A. BCA

Although the BCA approximation gives exactly the correct  $t = 0$  value of the memory function, this approximation leads to correlation functions that oscillate rapidly and with sharply increasing magnitude as  $t \rightarrow \infty$ . Although the shape of the BCA memory function looks reasonable, there is insufficient area under the curve for the solution to the kinetic equation to be well-behaved. We suspect that this is related to its failure to satisfy the symmetry property discussed in Appendix A. (Recall the form of this approximation, eqs. (2)–(8).)



## B. STA, MGBE, and K-MGBE

### 1. STA

Overall, for the high densities studied, the STA approximation does reasonably well at predicting correlation functions at all temperatures and wave vectors, with increasing quantitative accuracy with high temperature and large wave vector. The short time predictions of the STA are reasonably accurate, as is the overall longer time behavior. The STA approximation is able to reproduce qualitative trends of the various correlation functions with changes in wave vector. The trends with changes in temperature are also reproduced, except for the SLCC curve where the shifting and increasing magnitude of the negative dip is not well reproduced. In fact, the STA approximation consistently fails to predict the temperature dependence of the negative dips in the SLCC curve. A complete discussion of the results of the STA approximation can be found in Refs. 43 and 48.

### 2. MGBE

The MGBE approximation is more accurate at short times than the STA, as shown in Fig. 3, and is in essentially perfect agreement with the simulation data for times less than about 0.1. This statement holds for the self correlation functions at all temperatures and wave vectors studied. The short time part of the SLCC function is largely determined by the value of the  $\hat{k}\hat{k}$  matrix element of the memory function at  $t = 0$ . The MGBE does not have exactly the correct zero time values of the memory function matrix elements but it is more accurate than the STA, and this accounts for its accuracy at short times. The MGBE result begins to become inaccurate at  $t \approx 0.1$ , rising significantly above the simulation data.

For longer times,  $t \geq 0.1$ , the MGBE gives very inaccurate results. See Figs. 4 and 5. For large wave vectors at both high and low temperatures, the MGBE behaves reasonably, with a single minimum in the SLCC at approximately the right time, but an overall quantitative disagreement with the data. For small wave vectors at all temperatures, it predicts oscillation in the SLCC for times of about 0.2-0.3, a positive maximum in the function at  $t \approx 0.3$ , and a very slow decay of the correlation function to zero from above, in qualitative disagreement with the simulation results. The latter have a single minimum, followed by an approach to zero from below on a shorter time scale than the MGBE result approaches zero.

The origin of this unusual behavior, especially the oscillations, is easily understood from the nature of the MGBE. The memory function in the MGBE is a time correlation function for derivatives of the potential of mean force in a two particle system for which the two particles interact according to the potential of mean force of the fluid and move according to Hamiltonian dynamics. See

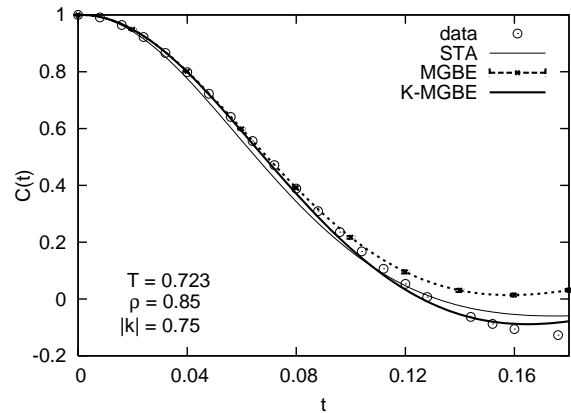


FIG. 3: Normalized SLCC function. Although the MGBE and K-BCA approximations do poorly at representing the simulation result for longer times, for times  $t < 0.1$  we see that these are the most quantitatively accurate approximations. The statistical error bars for the MGBE correlation function are shown and are barely discernible on this scale. All of the theoretical correlation functions have similarly small statistical errors.

eqs. (2), (10), (12) and Appendix C. This idea, which follows from the explicit formula eq. (12), is the basis for the algorithm used to evaluate the matrix elements of the memory function. The potential of mean force at high density is oscillatory and extends to distances of several atomic diameters. Thus, collisions that are relevant for the MGBE are of long duration and the correlation function that gives the memory function is nonzero for a very long time.

Figure 6 shows the time dependence of the principal matrix element of the memory function for the MGBE approximation for a low temperature state. There is a pronounced oscillation that persists for times longer than the time scale for the true correlation function to decay. For comparison, the STA memory function decays to zero very quickly, within times of the order of 0.1. As we shall discuss below in the next section, the large positive feature in the memory function and the subsequent oscillation are not present in the actual memory function.

These results show that the MGBE approximation, although quantitatively correct at short times, is qualitatively incorrect at intermediate and long times.

### 3. K-MGBE

The collisions described above that are the basis of the MGBE approximation, namely Hamiltonian dynamics of a pair of particles whose interaction potential is equal to the potential of mean force of the liquid, seem inappropriate for determining the dynamics of a dense liquid. The particles surrounding a pair of particles should do more to determine the dynamics of the particle pair than merely to renormalize the bare potential into the poten-

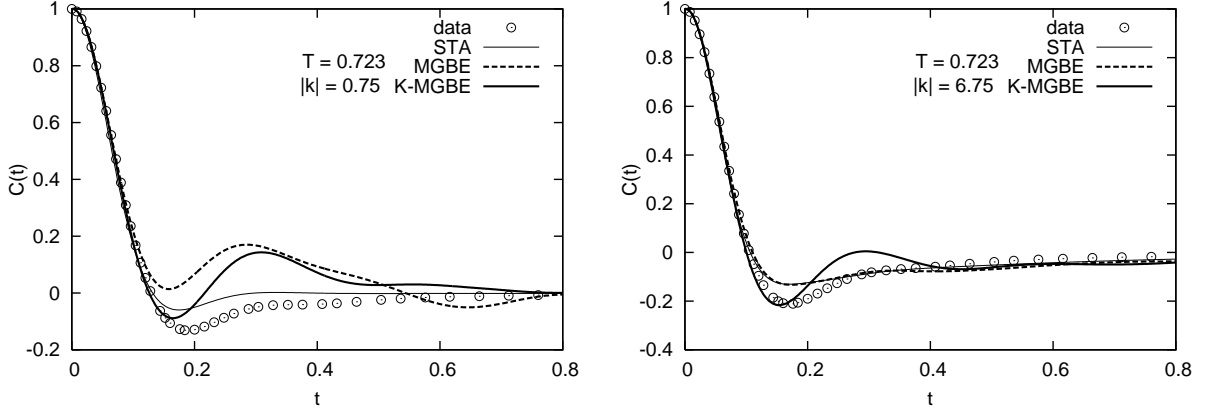


FIG. 4: Normalized SLCC function for the STA, MGBE and K-MGBE approximations for  $T = 0.723$  at small and large wave vector. The STA and MGBE curves lie on top of each other at large wave vector. High temperature results are shown in Fig. 5.

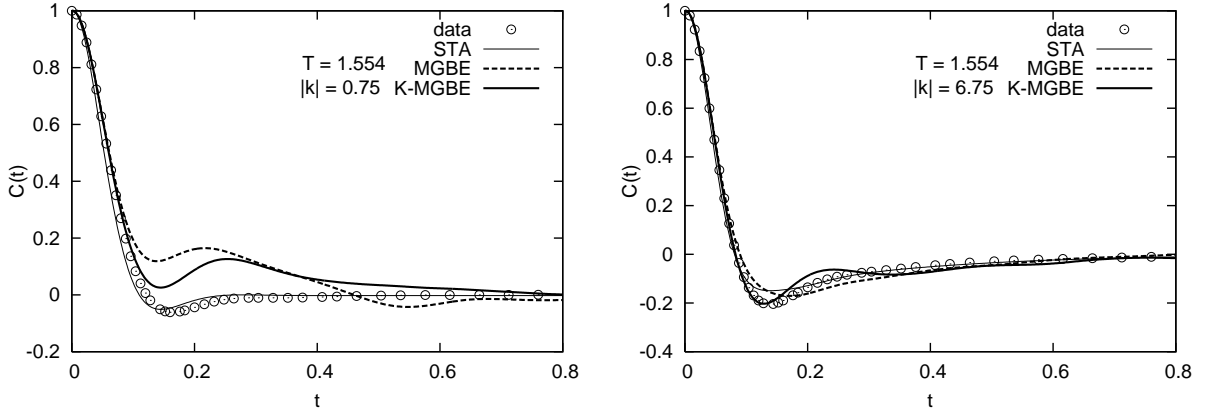


FIG. 5: Normalized SLCC results for the STA, MGBE, and K-MGBE approximations for  $T = 1.554$  at small and large wave vector. See Fig. 4 for low temperature results.

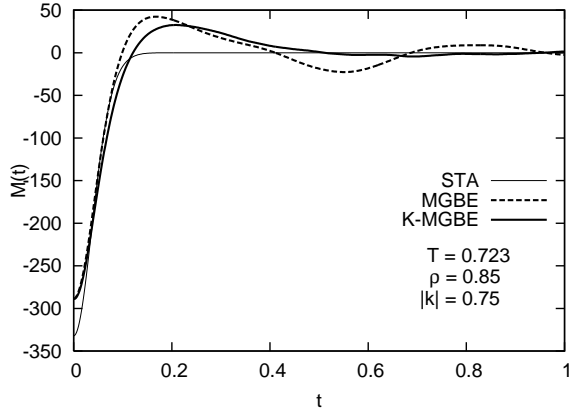


FIG. 6: Self part of the  $\hat{k}\hat{k}$  matrix element of the memory function. The STA approximation generates a non-oscillatory memory function while both MGBE and K-MGBE approximations yield oscillatory memory functions. These oscillations are the cause of the oscillations in the MGBE and K-MGBE results for the SLCC.

tial of mean force. In Mazenko's theory, this would be taken into account by including the quantity called  $\Gamma$ , which represents renormalized dynamical interactions of the pair. In the cluster theory, this would be taken into account by including the coupling of the pair to fluctuations of the density of third particles.

The K-MGBE approximation discussed above provides a tractable way of including these interactions, provided they are regarded as independent uncorrelated repulsive collisions of the two particles with third particles, approximated using the BGK model memory function. This approximation sums, in an approximate way, a class of diagrams in the exact diagrammatic theory. We assume that these collisions involve the short range repulsive part of the interatomic potential, so we pick the parameter  $\nu$  so that the BGK memory function has a strength that is related to that of the STA memory function. Since the most important matrix element of the memory function is the  $\hat{k}\hat{k}$  matrix element, we choose  $\nu$  so that this matrix element for the BGK model corresponds to the actual matrix element for the STA. More precisely, we choose  $\nu$

such that

$$\nu = \int_0^\infty dt' \hat{M}_{\hat{k}\hat{k},STA}^{(s)}(\mathbf{0}, t') \quad (13)$$

While this is a crude approximation overall, it was devised to give some idea of the effects of third particles on the dynamics of the pair, in the hope of yielding an improved version of the MGBE.

Figure 6 shows that the K-MGBE memory function has less pronounced oscillations and a more rapid decay to zero than the MGBE memory function. Figures 4 and 5 show the SLCC correlation functions given by the K-MGBE approximation. Introducing the BGK collisions extends the initial time interval over which the approximation is valid, for low and high temperatures and for small and large wave vector. The intermediate time behavior of the K-MBGE is unsatisfactory, however, with a peak in the correlation function at times of about 0.3 appearing under all conditions studied. The long time behavior of the K-MGBE is at best a slight improvement over that of the MGBE.

### C. Additional approximations

In an attempt to find improved binary collision approximations, we investigated a number of other possibilities.

*a. RPMF approximation.* The STA memory function, which uses the repulsive part of the potential in each of the vertices, has the virtue of decaying to zero rapidly without oscillations at long time that produce unphysical behavior of the correlation function at long times. The rapid decay is a result of the fact that the two particle dynamics in the calculation of the memory function involves purely repulsive interactions (and hence brief collisions) and the range of the repulsive potential is so short.

An approximation, which we denote RPMF, based on using the repulsive part of the potential of mean force in each vertex, was constructed and studied. While the memory function generated by this approximation has the feature of rapid decay, as discussed for the STA, its magnitude and its integrated area are smaller than that of the STA and it generates an SLCC that falls from its initial value significantly more slowly than the STA result. This basic flaw in the RPMF approximation is evident in the zero time value of the memory function (see Table I).

*b. K-RPMF approximation.* The K-RPMF approximation adds BGK collisions with third atoms to the RPMF approximation. This memory function decays more slowly than that of the RPMF, but it has the same initial value as the RPMF, and overall is not a significant improvement over the RPMF.

*c. A hybrid of the MGBE and STA approximations.* We attempted to construct approximations that have accurate values of the memory function at zero time but that were based on relatively brief collisions. In one such

approximation, we used the potential of mean force in the  $Q_{12}^{(c,1)}$  vertex and the  $Q_{21}^{(c,1)}$  vertex (as in the MGBE approximation) but the repulsive part of the potential in the  $Q_{22}^{(c,1)}$  vertex (as in the STA). We also considered the approximation that supplemented this approximation with BGK collisions with third particles. This hybrid is not a significant improvement over the MGBE or STA approximations and had some artifacts for small wave vector that are inconsistent with the simulation results.

*d. Other approximations.* A variety of other unsuccessful approximations were also studied. See Ref. 48 for details.

## V. EXTRACTION OF THE MEMORY FUNCTION

Thus far, we have tested approximate kinetic theories by calculating their memory functions, solving the memory function equation for the related correlation functions, and comparing the predicted correlation functions with computer simulation results. These comparisons give only an indirect test of the accuracy of the approximate memory function approximations.

In this section we consider a different set of questions. Given a correlation function calculated from simulation data, what is the memory function that corresponds to it? What are the properties of the ‘exact’ memory function? How do the approximate memory functions compare with the ‘exact’ memory function?

The numerical technique we use for extracting the memory function from the correlation function data employs a Fourier series representation of the memory function as a function of time. The Fourier coefficients in the series were adjusted to minimize the differences between the SLCC calculated from the memory function and the SLCC obtained from computer simulation. For small wave vector, the  $\hat{k}\hat{k}$  matrix element of the memory function plays the dominant role in determining the SLCC function.<sup>48</sup> The reason for this is that the coupling of the correlation function to other elements of the memory function involves positive powers of the wave vector. Thus we need to construct a Fourier representation of only this matrix element of the memory function and solve for the Fourier coefficients of just one function rather than many. The coefficients are found by a minimization of the sum of the squares of the deviations of the calculated correlation function and the simulated function. See Ref. 48 for details.

The extracted  $\hat{M}_{\hat{k}\hat{k}}^{(s)}(\mathbf{k}, t)$  for small wave vector is shown in Fig. 7 for the lowest and highest temperatures studied, where they are compared with the STA predictions for the same function. The extracted memory function at low temperature has none of the oscillations and high maxima that are predicted by the MGBE and K-MGBE approximations. Compare Fig. 6. The STA results are qualitatively similar to the extracted results, but there are significant differences. 1. The magnitude at zero time

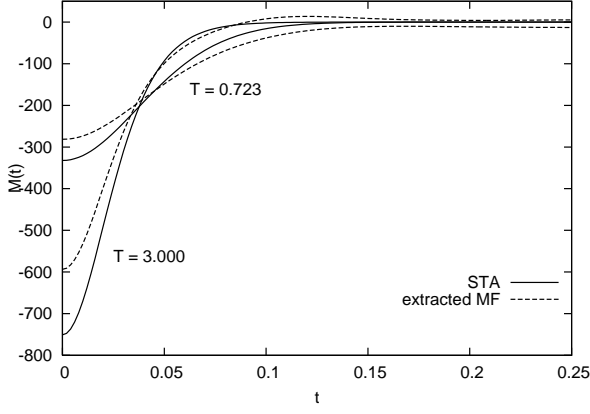


FIG. 7: Extraction results (dashed lines) for the  $\hat{k}\hat{k}$  matrix element of the self memory function compa STA curves (solid lines) at  $\rho = 0.85$  and  $|\mathbf{k}| = 0.75$ . The top set of lines at  $t = 0$  corresponds to  $T = 0$ . The lower set at  $t = 0$  corresponds to  $T = 3.000$ .

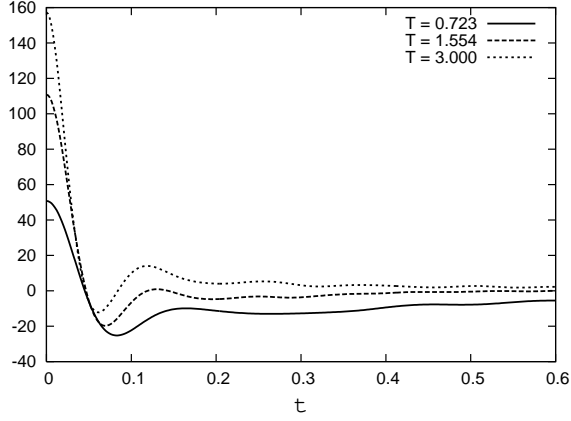


FIG. 8: The difference between the extracted and STA memory functions,  $\hat{M}_{kk,STA}(0.75, t) - \hat{M}_{kk,ext}(0.75, t)$ , for three different temperatures.

is larger for the STA than for the extracted memory function. 2. The STA curves fall rapidly to zero, while the extracted curves decay to zero more slowly, from above at the higher temperature, and from below at lower temperatures.

The differences between the extracted memory function and the STA approximation is plotted for high, medium, and low temperatures in Fig. 8. At the highest temperature, the memory function decays to zero from above. This is presumably a manifestation of the hydrodynamic vortex effect that is seen for hard spheres.<sup>57</sup> The long time negative part of the memory function at lower temperatures is presumably a manifestation of the cage effect, and is related to the long slow decay of the simulation correlation function at low temperature and small wave vector (see Fig. 4). The very long time part of the memory function is shown in Fig. 9.

The actual memory function at low temperatures

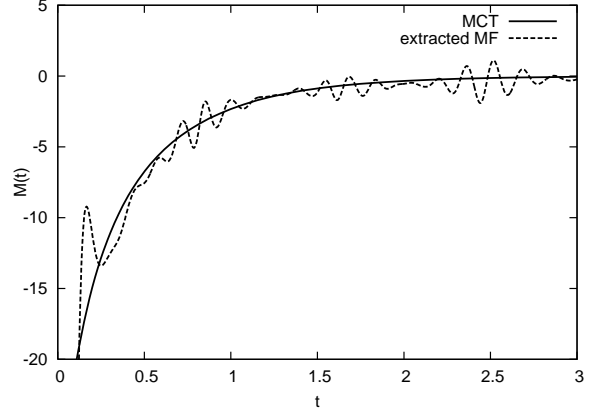


FIG. 9: The longer time part of the memory function predicted by mode coupling theory is compared to the memory function numerically extracted from the simulation data for the SLCC at  $T = 0.723$  and  $|\mathbf{k}| = 0.75$ .

clearly has a rapidly decaying part, falling to 2% of its initial value at  $t \approx 0.5$ , and a more slowly decaying part that falls to zero (within the statistical error) at about  $t = 1.5$ . None of the binary collision approximations we have studied is qualitatively consistent with the true long time behavior of the memory function. Moreover, none of them provides a quantitative description of the initial rapid decay.

## VI. MODE COUPLING DESCRIPTION OF THE LONG TIME PART OF THE MEMORY FUNCTION

The mode coupling theory of Götze<sup>58</sup> can be used to calculate, among other things, a correlation function denoted  $\phi_q^{(s)}(t)$  that is proportional to  $\hat{C}_{00}^{(s)}(\mathbf{k}, t)$ , the Fourier transform of a specific matrix element of  $C^{(s)}(11', t)$ . The theory is based on the Mori-Zwanzig projection operator method,<sup>59</sup> which relates this function to its second order memory function, denoted  $M_q^{(s)}(t)$ . The assumptions of the theory lead to a mode coupling relationship that expresses the long time part of  $M_q^{(s)}(t)$  as a bilinear functional of  $\phi_q^{(s)}(t)$  and  $\phi_q(t)$ , where the latter is proportional to  $\hat{C}_{00}^{(s)}(\mathbf{q}, t)$ . See eq. (3.34) of Ref. 58.

The kinetic theory presented here relates  $\hat{C}_{00}^{(s)}(\mathbf{k}, t)$  to an infinite dimensional matrix of memory functions  $\hat{M}_{\mu\nu}^{(s)}(\mathbf{k}, t)$ . For small wave vector  $\mathbf{k}$ ,  $\hat{C}_{00}^{(s)}(\mathbf{k}, t)$  is coupled primarily to  $\hat{M}_{kk}^{(s)}(\mathbf{k}, t)$ , and in the limit as this wave vector goes to zero, this is the only element that affects the value of  $\hat{C}_{00}^{(s)}(\mathbf{k}, t)$ . Our numerical work confirms that  $|\mathbf{k}| = 0.75$  is small enough for this to be the case. It is straightforward to show that when this is the case, the relationship between  $\hat{M}_{kk}^{(s)}(\mathbf{k}, t)$  and  $\hat{C}_{00}^{(s)}(\mathbf{k}, t)$  is precisely of the form generated by the Mori-Zwanzig theory.

In other words, for small wave vector, the single matrix element  $\hat{M}_{\hat{k}\hat{k}}^{(s)}(\mathbf{k}, t)$  is the Mori-Zwanzig second order memory function of  $\hat{C}_{\hat{0}\hat{0}}^{(s)}(\mathbf{k}, t)$ .

When the mode coupling relationship mentioned above is expressed in terms of the present kinetic theory, the result is of the following form

$$\hat{M}_{\hat{k}\hat{k}}^{(s)}(\mathbf{k}, t) = \int d\mathbf{q} A(\mathbf{k}, \mathbf{q}) \hat{C}_{\hat{0}\hat{0}}(\mathbf{q}, t) \hat{C}_{\hat{0}\hat{0}}^{(s)}(\mathbf{k} - \mathbf{q}, t)$$

where  $A(\mathbf{k}, \mathbf{q})$  is a nonnegative function. The mode coupling theory asserts that this holds for times longer than the duration of brief binary collisions, which in the present theory corresponds roughly to the time at which the STA memory function has decayed to zero.

Applying this result to  $|\mathbf{k}| = 0$ , we find

$$\hat{M}_{\hat{k}\hat{k}}^{(s)}(\mathbf{0}, t) = \int d\mathbf{q} A(\mathbf{0}, \mathbf{q}) \hat{C}_{\hat{0}\hat{0}}(\mathbf{q}, t) \hat{C}_{\hat{0}\hat{0}}^{(s)}(\mathbf{q}, t) \quad (14)$$

Each of the two time dependent functions on the right depends on the magnitude, but not the direction, of its wave vector argument. The function  $A(\mathbf{0}, \mathbf{q})$  is zero if  $|\mathbf{q}| = 0$ , small near  $|\mathbf{q}| = 0$ , and highly peaked near  $|\mathbf{q}| = q_{max} \approx 2\pi/\sigma$ . Assuming that the integral above is dominated by the range of wave vectors whose magnitude is near this value, we find

$$\hat{M}_{\hat{k}\hat{k}}^{(s)}(\mathbf{0}, t) \approx (\text{constant}) \times \hat{C}_{\hat{0}\hat{0}}(q_{max}, t) \hat{C}_{\hat{0}\hat{0}}^{(s)}(q_{max}, t) \quad (15)$$

where the constant is positive. Since  $\hat{M}_{\hat{k}\hat{k}}^{(s)}(\mathbf{k}, t)$  is an even differentiable function of the wave vector argument, it is very slowly varying near  $|\mathbf{k}| = 0$ , and we will apply this result for  $|\mathbf{k}| = 0.75$ , the smallest nonzero wave vector studied in this work.

We can test this relationship by comparing the time dependence of the extracted  $\hat{M}_{\hat{k}\hat{k}}^{(s)}(0.75, t)$  obtained from the simulation data with the time dependence of the right side of eq. (15), which contains functions that are routinely obtained from simulation data. Figure 9 shows the extracted memory function  $\hat{M}_{\hat{k}\hat{k}}^{(s)}(0.75, t)$  for longer times ( $t > 0.1$ ) for the lowest temperature studied. At that time, the STA memory function has decayed almost completely to zero. The extracted memory function has oscillations that are an artifact of the extraction procedure (note the vertical scale compared with the graph of Fig. 7). Figure 9 also shows the right side of eq. (15), with the constant chosen so that the results matches the value of the extracted memory function for  $t \approx 1$ . With this choice of the constant, the time dependence of the right side accounts remarkably well for the time dependence of the memory function matrix element.

Note that this test was only for the smallest wave vector at the lowest temperature studied. For high temperatures, eq. (15) is qualitatively incorrect (*i.e.*, the predicted sign of the memory function is incorrect). This is presumably because the behavior is dominated by a hydrodynamic vortex effect,<sup>57</sup> rather than the cage effect

described by mode coupling theory. For higher wave vectors at low temperatures, the test cannot be performed, since the simple relationship between  $\hat{M}_{\hat{k}\hat{k}}^{(s)}(\mathbf{k}, t)$  and the second order memory function of the Mori-Zwanzig theory does not hold. Note, also, that mode coupling theory allows, in principle, the calculation of the constant of proportionality, but we have not done this. Nevertheless, the agreement in Fig. 9 is striking, suggesting that mode coupling theory accounts quantitatively for the time dependence of the memory function for long times (*i.e.*, for times longer than the time of a brief binary collision) for the lowest temperature studied, which corresponds to the liquid state near the triple point.

## VII. SUMMARY AND CONCLUSIONS

### *a. The accuracy of various approximate theories.*

We have investigated various binary collision approximations for the memory function of the correlation function of density fluctuations in a dense Lennard-Jones liquid at equilibrium and compared their predictions with computer simulation results for the self correlation functions, especially the self longitudinal current correlation function (SLCC).

The BCA of Ranganathan and Andersen is exact at  $t = 0$ , but it leads to divergent results at long times, presumably because of its failure to satisfy important symmetry properties.

The moderate density approximation of the generalized Boltzmann-Enskog memory function (MGBE) of Mazenko and Yip<sup>36</sup> is accurate at very short times. However, its intermediate time behavior is very different from the correct results, and its predicted correlation functions display unphysical oscillations at intermediate times.

The STA of Ranganathan and Andersen<sup>42,43</sup> is not exact at  $t = 0$ . It describes the initial drop of the SLCC to zero reasonably accurately, but it does not accurately describe the shape and depth of the minimum in that function and its temperature dependence. At high temperatures, it gives accurate values of the transport coefficients.<sup>43</sup>

The K-MGBE approximation, which introduces uncorrelated brief collisions of the colliding pair with third particles, is more accurate than the MGBE at short times but its intermediate time behavior is still very inaccurate.

No other binary collision approximation discussed in this paper is a systematic improvement over the STA.

### *b. The behavior of the extracted memory function.*

For small wave vector, the most important matrix element of the memory function can be extracted from the simulation results for the SLCC.

At short time, the extracted memory function drops rapidly to values close to zero, in a way similar to the STA result, and then has a very small, long-lived, nonoscillatory tail that is positive at high temperatures and negative at low temperatures. At low temperatures, the negative tail is important for determining the shape of the

minimum in the SLCC. This tail is probably the result of physical effects that are not included in any binary collision approximation. The time dependence of the long time tail of the memory function is in striking agreement with what is predicted by mode coupling theory, but this is only a limited confirmation of that theory since the extracted memory function can be obtained only at small wave vector.

*c. Conclusions and speculations.* The negative feature of the SLCC for the dense Lennard-Jones fluid indicates that the velocity of a particle is anticorrelated with its velocity at times that are more than about 0.1 time units earlier. An important part of the basis for this feature can be described by binary collision theories that take into account the finite duration of very repulsive collisions. For hard spheres, the short time feature of the memory function is a Dirac delta function, which by itself would generate monotonic decay of the SLCC from above. In the STA, the short time feature is spread over a range of times of the order of the duration of a repulsive collision, and the resulting correlation function has a negative dip. However, the increase of the depth of the negative feature as the temperature is lowered is caused not by this short time feature but rather by a small, negative, temperature dependent long time tail in the memory function. This is presumably a manifestation of what is commonly regarded as caging of atoms at low temperatures and cannot be described by binary collision approximations. Instead, mode coupling theory or something else that goes beyond binary collision approximations is needed to describe this aspect of the negative feature.

This conclusion is not at all surprising. Theories that use mode coupling commonly include a binary collision term in the memory function but do not discuss in detail the nature of that term. It is clear from the present work that the short time part of the memory function has behavior associated with brief binary *repulsive* collisions, such as those described by the STA. Collisions that include attractive as well as repulsive interactions, such as those of the MGBE, have a much longer duration, and theories that include them have memory functions that decay to zero much too slowly to provide a good first approximation for the correlation functions at intermediate times.

We have not been able to derive any binary collision theory that describes brief binary repulsive collisions and that has exactly the correct value of the memory function at  $t = 0$ . There is a straightforward expression for the zero time value of the memory function<sup>60</sup> in terms of static correlation functions, and this expression involves the entire potential, the entire potential of mean force, and the pair correlation function. Any graphical approximation for the memory function that includes all this at  $t = 0$  would have more physics in it than binary repulsive collisions.

This leads us to speculate that the memory function for density fluctuations can be usefully regarded as a sum of

at least three parts: a contribution from repulsive binary collisions (the STA or something similar to it), another short time part that is related to all the other interactions (but whose nature is not understood), and a longer time slowly decaying part that describes caging (of the type predicted by mode coupling theory).

### Acknowledgments

The authors would like to thank Dr. Thomas Young and Richard Stein for providing the molecular dynamics data used in this work. This work was supported by the National Science Foundation grant CHE-0408786. One of the authors (J.N.-V.) would like to acknowledge support from a DOE CSGF fellowship.

### APPENDIX A: SYMMETRY PROPERTIES OF THE MEMORY FUNCTION

The theory we are discussing describes a system with a time independent Hamiltonian at equilibrium. The exact correlation function for the system must satisfy symmetry properties related to stationarity and time reversal invariance. Stationarity implies

$$C^{(s)}(\mathbf{R}_1, \mathbf{P}_1; \mathbf{R}'_1, \mathbf{P}'_1; t) = C^{(s)}(\mathbf{R}'_1, \mathbf{P}'_1; \mathbf{R}_1, \mathbf{P}_1; -t) \quad (\text{A1})$$

A combination of time reversal symmetry and stationarity implies

$$C^{(s)}(\mathbf{R}_1, \mathbf{P}_1; \mathbf{R}'_1, \mathbf{P}'_1; t) = C^{(s)}(\mathbf{R}'_1, -\mathbf{P}'_1; \mathbf{R}_1, -\mathbf{P}_1; t)$$

There are similar implications for other correlation functions and for the memory function. The importance of related symmetry conditions formulated in the Laplace transform domain have been emphasized by Mazenko.<sup>36</sup>

The exact diagrammatic series satisfies these relationships exactly. This follows from the fact that the series are formally exact, but it can also be proven directly from the topological structure of the diagrams and the symmetry properties of the vertices and bonds that appear in the diagrams. (The diagrammatic theory was derived<sup>39,40,41,42,43</sup> only for positive time arguments. However, the results can easily be extended to negative time by analytic continuation in order to verify that they satisfy eq. (A1).)

Graphical approximations are constructed by retaining a subset of diagrams in the exact series and/or by making approximations for the vertices. Such graphical approximations may or may not satisfy the symmetry requirements, depending on the nature of the subset retained and details of the approximations made.

We have not been able to formulate a useful set of necessary conditions that a general graphical approximation must satisfy in order to be consistent with the symmetry properties. However, various sets of sufficient conditions can be formulated and proven. In particular,

two sets of sufficient conditions for a binary collision approximation, of the class discussed above, to satisfy the symmetry property can be stated. The sufficient conditions reduce to conditions on the quantities that appear in the vertices. The details will be omitted here and we shall merely quote the results. 1. The MGBE approximation for  $M^{(s)}$  satisfies the symmetry conditions exactly. 2. The BCA approximation for  $M^{(s)}$  does not satisfy the known sufficient conditions for symmetry. It is likely that it strongly fails to satisfy the symmetry, and this is probably the reason why it is such a poor approximation at long times. 3. The STA approximation for  $M^{(s)}$  does not satisfy either set of known sufficient conditions for symmetry exactly. However, in the limit in which the repulsive forces become hard sphere forces, it does satisfy one set. Thus for very strong repulsive forces it is at least numerically close to satisfying the symmetry conditions. 4. The RPFM approximation for  $M^{(s)}$  satisfies the symmetry conditions exactly. 5. The hybrid approximation discussed above does not satisfy either set of known sufficient conditions for symmetry exactly. 6. If a binary collision approximation satisfies either of the two known sets of sufficient conditions, its  $K$  approximation satisfies the symmetry conditions exactly. Thus the K-MGBE and K-RPFM satisfy the symmetry properties exactly.

## APPENDIX B: TWO FORMS OF THE LEFT VERTEX IN THE MEMORY FUNCTION

*a. The left vertex in the MGBE and BCA.* The reasoning that leads to the derivation of the MGBE approximation in the context of the Mazenko theory and the BCA in the context of the graphical theory are very similar, but the results are slightly different. The nature of the difference is discussed in this appendix.

The graphical theory contains a vertex  $Q_{12}(1; 1'2')$  defined as

$$Q_{12}(1; 1'2') \equiv \frac{1}{2!} \int d1''d2'' W_{12}(1; 1''2'') K_2(1''2''; 1'2') \quad (\text{B1})$$

$$= (1 + \mathcal{I}(1'2')) \nabla_{\mathbf{R}} u(12') \cdot \nabla_{\mathbf{P}} \delta(11') \quad (\text{B2})$$

(See eq. (3) and Sec. III of Ranganathan and Andersen<sup>42</sup> and Appendix A.4 of Andersen.<sup>40</sup> Here the  $\mathcal{I}$  operator interchanges the two arguments in the subsequent expression.) The first equality is a definition. The second equality represents an exact evaluation. Although this function has three arguments, they represent only two distinct particles, since the Dirac delta function in each term clearly indicates that the left argument corresponds to the same particle as one of the right arguments. So this vertex appears appropriate for a theory that includes binary collisions between particles.

An exact evaluation of  $W_{12}(1; 1'2')$  gives two terms.

The first term is

$$W_{12}(1; 1'2')_{\text{first term}} = -(1 + \mathcal{I}(1''2'')) n(1'') n(2'') \\ \times M_m(1'') M_m(2'') g(1''2'') \nabla_{\mathbf{P}} \delta(1''1) \cdot \nabla_{\mathbf{R}} v_{MF}(1''2'')$$

It clearly represents two distinct particles. The second term (not given here), which is very complicated, involves static correlations functions for three distinct particles.

An exact evaluation of  $W_{12}(1; 1'2')$  gives two terms. The first term is

$$W_{12}(1; 1'2')_{\text{first term}} = -(1 + \mathcal{I}(1''2'')) n(1'') n(2'') \\ \times M_m(1'') M_m(2'') g(1''2'') \nabla_{\mathbf{P}} \delta(1''1) \cdot \nabla_{\mathbf{R}} v_{MF}(1''2'')$$

This clearly represents two distinct particles. The second term (not given here), which is very complicated, involves static correlations functions for three distinct particles.

An exact evaluation of  $K_2(1''2''; 1'2')$  also gives two terms. The first term is

$$K_2(1''2''; 1'2')_{\text{first term}} = \frac{(1 + \mathcal{I}(1''2'')) \delta(1''1') \delta(2''2')}{n(1) M_m(1) n(2) M_m(2) g(12)} \quad (\text{B3})$$

This term describes two distinct particles. The second term involves static correlations functions for more than two distinct particles.

In the spirit of a binary collision approximation, it would be reasonable to approximate both  $W_{12}$  and  $K_2$  by their first terms. If this is done and the results are used in (B1), we get the following approximate result.

$$Q_{12}(1; 1'2') \approx (1 + \mathcal{I}(1'2')) \nabla_{\mathbf{R}} v_{MF}(12') \cdot \nabla_{\mathbf{P}} \delta(11') \quad (\text{B4})$$

which is of the same form as the exact result but with the potential replaced by the potential of mean force.

Mazenko's theory contains quantities analogous to  $W_{12}$  and  $K_2$ . In the derivation of the MGBE, the contributions that correspond to more than two distinct particles are not included in each of these two functions. This would be analogous to using eq. (B4) rather than (B2). This is the origin of the fact that the final expression for the MGBE differs from the BCA in the way shown in eqs. (9) and (10). It is only in the factor of  $Q_{12}$  that restricting attention to two particle effects leads to different results depending on whether the  $Q$  vertices or the separate  $W$  and  $K$  functions are regarded as the quantities that are to be expressed in terms of two particle contributions.

*b. Two comments.* 1. The use of the exact result for  $Q_{12}$  in the BCA is the origin of the fact that the BCA does not have the symmetry properties discussed in Appendix A. The matter of whether an approximation satisfies the symmetry properties is determined by the relationships among all the approximations made rather than the accuracy of individual approximations. 2. This difference between the left vertices of the two theories (with the bare potential being replaced by a factor of the

potential of mean force) appears similar to differences noted in approximate kinetic theories of hard spheres<sup>34,61</sup> and of plasmas.<sup>62,63,64,65</sup> The plasma case may be related to the present situation but is more complicated in that both the left and right vertices are different in various versions of the theory. The similarity to the hard sphere case is superficial, since the latter involves having different numbers of factors of  $g(d)$ , the pair correlation function of hard spheres at contact, in the memory function. A factor of the pair correlation function cannot arise from replacing the bare potential by the potential of mean force. The differences in the hard sphere kinetic theories appear more closely related to approximating  $K_2$  by the first term in eq. (B3) and then approximating the latter by its ‘disconnected’ approximation

$$\begin{aligned} K_2(1''2''; 1'2')_{\text{first term disconnected}} \\ = \frac{(1 + \mathcal{I}(1''2'')) \delta(1''1') \delta(2''2')}{n(1)M_m(1)n(2)M_m(2)} \end{aligned}$$

which is equivalent to multiplying the approximate  $K_2$  by a factor of the pair correlation function  $g$ .

### APPENDIX C: NUMERICAL CALCULATION OF THE MATRIX ELEMENTS OF THE MEMORY FUNCTION AND CORRELATION FUNCTIONS

The matrix elements of the memory function can be expressed as an ensemble average over a two particle probability distribution function as follows

$$\hat{M}_{\vec{\mu}\vec{\nu}}(\mathbf{k}, t) = \langle W_{\vec{\mu}\vec{\nu}}(\mathbf{k}, t; 12) \rangle \int_0^{r_c} dr 4\pi r^2 g(r)$$

where  $r_c$  is the cutoff distance associated with the potential governing the dynamics, that is  $V_{22}$ , and the quantity being averaged is

$$\begin{aligned} W_{\vec{\mu}\vec{\nu}}(\mathbf{k}, t; 12) = & \nabla V_{Q_{21}}(\mathbf{R}) \cdot \nabla h_{\vec{\nu}}(\mathbf{P}_1) \\ & \times \nabla V_{Q_{12}}(|\mathbf{R}_{ab}|) \cdot [e^{-i\mathbf{k}\cdot\mathbf{R}_a} \nabla h_{\vec{\mu}}(\mathbf{P}_a) - e^{-i\mathbf{k}\cdot\mathbf{R}_b} \nabla h_{\vec{\mu}}(\mathbf{P}_b)] \end{aligned}$$

The meaning of phase points  $a$  and  $b$  are described in Sct. III A. The first term in brackets gives the self part of the memory function, while the second term gives the distinct part. Both terms together constitute the total memory function. The two particle distribution function required for calculation of the average  $\langle W_{\vec{\mu}\vec{\nu}}(\mathbf{k}, t; 12) \rangle$

$$P^{[2]}(12) \propto \rho M_m(\mathbf{P}_1) M_m(\mathbf{P}_2) \delta(\mathbf{R}_1) g(\mathbf{R}_2) \Theta(r_c - |\mathbf{R}_2|)$$

The average of  $W$  over this distribution is calculated by the two particle trajectory method of Ranganathan and Andersen.<sup>43</sup> In this method, the coordinates and momenta called 1, 2 are sampled from  $P^{[2]}$  and used as initial conditions for a two particle trajectory calculation from which the  $W$  quantities are calculated as functions of time. For most of the approximations, the trajectories are calculated using Hamiltonian mechanics of the

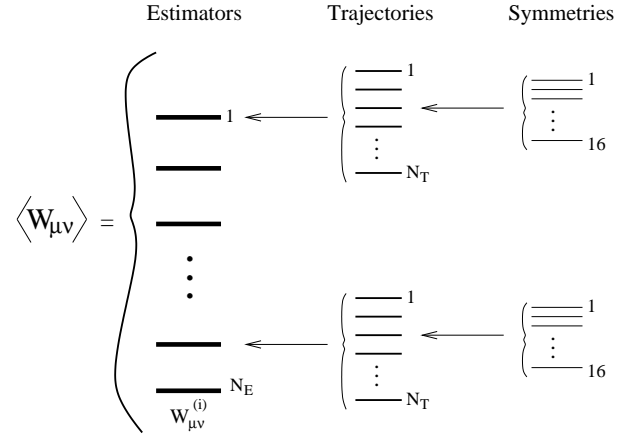


FIG. 10: A schematic representation of the averaging procedure for the matrix elements of the memory function.

two particles interacting via the potential  $V_{22}$ . For the  $K$  approximations, the dynamics are supplemented by an algorithm that includes the effect of the  $\tilde{L}_{BGK}$  in eq. (11). The algorithm gives each particle, at randomly chosen times, a new momentum chosen from a Boltzmann distribution, without changing its position. The time at which these interventions occur for each particle are uncorrelated with each other and occur with an average frequency  $\nu$  for each particle, where  $\nu$  is given by eq. (13).

The matrix elements of the memory function can be divided into four components: self real, distinct real, self imaginary, and distinct imaginary parts. Each part is computed for each matrix element in a calculation that takes advantage of a number of properties derived from the Hermite polynomial basis functions, the two particle problem, and the known  $t = 0$  values of the matrix elements themselves.

The basis function  $h_{\vec{0}}(\mathbf{P})$  is a constant. Since the gradients of the Hermite polynomial functions with respect to momenta, not the Hermite functions themselves, appear in the expression for the matrix elements of the memory function,  $\hat{M}_{\vec{0}\vec{\nu}}$  for all  $\vec{\nu}$  and  $\hat{M}_{\vec{\mu}\vec{0}}$  for all  $\vec{\mu}$  are identically zero for all time and need not be computed numerically.

The two particle trajectory method can be mapped onto a highly symmetric two particle scattering problem. The symmetry relations of most concern are the following. 1. If  $\mu_z + \nu_z$  is even, then the self and distinct imaginary parts are identically zero for all times. 2. If  $\mu_z + \nu_z$  is odd, then the self and distinct real parts are identically zero for all times. See Ref. 48 for the proofs of these properties.

Figure 10 is a schematic representation of the averaging procedure used to calculate the matrix elements of the memory function. For each pair of indices  $\vec{\mu}\vec{\nu}$ , the following calculation scheme was used. 1. A set of initial conditions is randomly sampled from the two particle probability distribution  $P^{[2]}$  and a molecular dynamics trajectory is computed by solving Hamilton’s equations



of motion. 2. This single trajectory is used to generate fifteen symmetry related two particle trajectories based on the  $D_{4h}$  symmetry of the two particle system. The values of the various parts of  $W_{\bar{\mu}\bar{\nu}}$  are calculated for each of the sixteen trajectories. This corresponds to generating numbers that appear in the rightmost column in Fig. 10. The sixteen sets of numbers are averaged together to give the first type of average for the various parts of  $W_{\bar{\mu}\bar{\nu}}$ . The values are entered into the middle column of the figure. 3. Steps 1 and 2 are repeated for a total of  $N_T$  times. The  $N_T$  results are averaged to give a second type of average, which is entered in the left column of the figure. 4. Steps 1-3 are repeated  $N_E$  times to yield a set of  $N_E$  values of the second type of average. These  $N_E$  values are averaged together to give a third type of average, however they are not given equal weight as in steps 2 and 3. In this case, we use a constrained reweighting method, based on a maximum likelihood principle, that adjusts the weights assigned to each of the  $N_E$  values such that the correct results are obtained for the calculated averages of the matrix elements at  $t = 0$ . The result of this process is a set of values for the real and imaginary parts of the self and distinct parts

of  $(W_{\bar{\mu}\bar{\nu}})$ . The values automatically satisfy the symmetry properties mentioned above, because of the way the symmetry related trajectories were used, and they automatically have the correct values at  $t = 0$ , because of the reweighting method. The latter automatically reduces the statistical error for small nonzero times as well. Details of this method can be found in Ref. 48. The self parts of the average are used in eq. (12) to give the desired matrix elements  $\hat{M}_{\bar{\mu}\bar{\nu}}^{(s)}$ . 5. The correlation functions of interest in this work,  $\hat{C}_{\bar{0}\bar{0}}^{(s)}(\mathbf{k}, t)$  and  $\hat{C}_{\bar{k}\bar{k}}^{(s)}(\mathbf{k}, t)$ , are computed by numerically solving the kinetic equation using the Euler method with the appropriate matrix elements of the memory function.

Steps 1-5 are repeated  $N_s$  times to generate  $N_s$  statistically independent results for the functions  $\hat{M}_{\bar{\mu}\bar{\nu}}(t)$  and for  $\hat{C}_{\bar{0}\bar{0}}^{(s)}(t)$  and  $\hat{C}_{\bar{k}\bar{k}}^{(s)}(t)$ . These  $N_s$  results for each function are averaged, and statistical error bars are computed in the usual way. The results presented in this paper are these average quantities. The values of  $N_T$ ,  $N_E$  and  $N_s$  used in this work are  $N_T = 100$ ,  $N_E = 1000$ , and  $N_s = 10$ .

- 
- \* Electronic address: hca@stanford.edu
- <sup>1</sup> Theories based on the idea of *uncorrelated* binary collisions are implemented by calculating a binary collision contribution to the memory function of a correlation function of interest, or alternatively, to the kinetic equation for the distribution function of interest. When such a memory function or kinetic equation is applied to the calculation of the correlation function, the result is a description of the effect of an arbitrary number of uncorrelated binary collisions. This is to be distinguished from binary collision theories that calculate the contribution of a single binary collision to the correlation function.
  - <sup>2</sup> Most of the detailed work on the theory of liquids deals with the special case of atomic liquids. We shall focus on this case, but most of the ideas and results can be generalized to more complicated fluids. Here we are concerned only with the case of liquids with short ranged interatomic potentials and forces.
  - <sup>3</sup> D. K. Hoffman and C. F. Curtiss, *Physics of Fluids* **7**, 1887 (1964).
  - <sup>4</sup> D. K. Hoffman and C. F. Curtiss, *Physics of Fluids* **8**, 667 (1965).
  - <sup>5</sup> D. K. Hoffman and C. F. Curtiss, *Physics of Fluids* **8**, 890 (1965).
  - <sup>6</sup> S. Chapman and T. G. Cowling, *The mathematical theory of non-uniform gases* (Cambridge University Press, Cambridge, England, 1970), 3rd ed.
  - <sup>7</sup> J. O. Hirschfelder, C. F. Curtiss, and R. B. Bird, *Molecular theory of gases and liquids* (Wiley, New York, 1964).
  - <sup>8</sup> S. A. Rice and A. R. Allnatt, *J. Chem. Phys.* **34**, 2144 (1961).
  - <sup>9</sup> A. R. Allnatt and S. A. Rice, *J. Chem. Phys.* **34**, 2156 (1961).
  - <sup>10</sup> H. T. Davis, S. A. Rice, and J. V. Sengers, *J. Chem. Phys.* **35**, 2210 (1961).
  - <sup>11</sup> J. Karkheck and G. Stell, *B. Am. Phys. Soc.* **25**, 349 (1980).
  - <sup>12</sup> J. Karkheck and G. Stell, *J. Chem. Phys.* **75**, 1475 (1981).
  - <sup>13</sup> J. Karkheck and G. Stell, *Phys. Rev. A* **25**, 3302 (1982).
  - <sup>14</sup> G. Stell, J. Karkheck, and H. van Beijeren, *J. Chem. Phys.* **79**, 3166 (1983).
  - <sup>15</sup> J. Karkheck, H. van Beijeren, I. de Schepper, and G. Stell, *Phys. Rev. A* **32**, 2517 (1985).
  - <sup>16</sup> J. Karkheck, G. Stell, and J. Xu, *J. Chem. Phys.* **89**, 5829 (1988).
  - <sup>17</sup> R. C. Castillo, E. Martina, M. L. de Haro, J. Karkheck, and G. Stell, *Phys. Rev. A* **39**, 3106 (1989).
  - <sup>18</sup> H. C. Longuet-Higgins and B. Widom, *Mol. Phys.* **8**, 549 (1964).
  - <sup>19</sup> H. Reiss, *Adv. Chem. Phys.* **9**, 1 (1965).
  - <sup>20</sup> B. Widom, *Science* **157**, 375 (1967).
  - <sup>21</sup> J. A. Barker and D. Henderson, *J. Chem. Phys.* **47**, 4714 (1967).
  - <sup>22</sup> J. A. Barker and D. Henderson, *Rev. Mod. Phys.* **25**, 587 (1967).
  - <sup>23</sup> J. D. Weeks, D. Chandler, and H. C. Andersen, *J. Chem. Phys.* **25**, 149 (1971).
  - <sup>24</sup> D. Chandler, J. D. Weeks, and H. C. Andersen, *Science* **220**, 788 (1983).
  - <sup>25</sup> J. L. Lebowitz, G. Stell, and S. Baer, *J. Math. Phys.* **6**, 1282 (1965).
  - <sup>26</sup> H. C. Andersen, D. Chandler, and J. D. Weeks, *J. Chem. Phys.* **57**, 2626 (1972).
  - <sup>27</sup> J.-P. Hansen and I. R. McDonald, *Theory of Simple Liquids* (Academic, London, 1986), 2nd ed.
  - <sup>28</sup> J. E. Mayer and M. G. Mayer, *Statistical Mechanics* (Wiley, New York, 1976), 2nd ed.
  - <sup>29</sup> T. Morita and K. Hiroike, *Prog. Theor. Phys.* **25**, 537

- (1961).
- <sup>30</sup> G. Stell, *The equilibrium theory of classical fluids; a lecture note and reprint volume* (W.A. Benjamin, New York, 1964), edited by H.L. Frisch and J.L. Lebowitz.
- <sup>31</sup> H. C. Andersen, *Statistical Mechanics* (Plenum Press, New York, 1977), vol. 1, edited by B.J. Berne.
- <sup>32</sup> G. F. Mazenko, T. Y. C. Wei, and S. Yip, *Phys. Rev. A* **6**, 1981 (1972).
- <sup>33</sup> G. F. Mazenko, *Phys. Rev. A* **7**, 209 (1973).
- <sup>34</sup> G. F. Mazenko, *Phys. Rev. A* **7**, 222 (1973).
- <sup>35</sup> G. F. Mazenko, *Phys. Rev. A* **9**, 360 (1974).
- <sup>36</sup> G. F. Mazenko and S. Yip, *Statistical Mechanics. Part B: Time-Dependent Processes* (Plenum, Inc., 1977), edited by B.J. Berne.
- <sup>37</sup> T. P. Young and H. C. Andersen, *J. Chem. Phys.* **118**, 3447 (2003).
- <sup>38</sup> T. P. Young and H. C. Andersen, *J. Phys. Chem. B* **109**, 2985 (2005).
- <sup>39</sup> H. C. Andersen, *J. Phys. Chem. B* **106**, 8326 (2002).
- <sup>40</sup> H. C. Andersen, *J. Phys. Chem. B* **107**, 10226 (2003).
- <sup>41</sup> H. C. Andersen, *J. Phys. Chem. B* **107**, 10234 (2003).
- <sup>42</sup> M. Ranganathan and H. C. Andersen, *J. Chem. Phys.* **121**, 1243 (2004).
- <sup>43</sup> M. Ranganathan and H. C. Andersen, *J. Phys. Chem.* **109**, 21437 (2005).
- <sup>44</sup> L. Verlet, *Phys. Rev. A* **2**, 2514 (1970).
- <sup>45</sup> L. Sjögren, *J. Phys. C: Solid State Phys.* **13**, 705 (1980).
- <sup>46</sup> L. Sjögren, *Phys. Rev.* **A22**, 2866 (1980).
- <sup>47</sup> L. Sjögren, *Phys. Rev.* **A22**, 2883 (1980).
- <sup>48</sup> J. E. Noah-Vanhoucke, Ph.D. thesis, Stanford University (2006).
- <sup>49</sup> See section IVB of Ref. 42.
- <sup>50</sup> See eqs. (78), (98), (220), and the related discussions in Ref. 36.
- <sup>51</sup> See eqs. (220)-(221) of Ref. 36.
- <sup>52</sup> P. L. Bhatnagar, E. P. Gross, and M. Krook, *Phys. Rev.* **94**, 511 (1954).
- <sup>53</sup> See eqs. (93)-(95) of Ref. 36.
- <sup>54</sup> M. Ranganathan, Ph.D. thesis, Stanford University (2003).
- <sup>55</sup> R. S. L. Stein, *unpublished simulation results*.
- <sup>56</sup> M. P. Allen and D. J. Tildesley, *Computer Simulation of Liquids* (Oxford University Press, 1989), 1st ed.
- <sup>57</sup> B. J. Alder and T. E. Wainwright, *Phys. Rev. A* **1**, 18 (1970).
- <sup>58</sup> W. Götze, *Liquids, Freezing, and the Glass Transition* (North-Holland, Amsterdam, 1991), edited by J.P. Hansen, D. Levesque, and J. Zinn-Justin.
- <sup>59</sup> H. Mori, *Phys. Rev.* **33**, 423 (1965).
- <sup>60</sup> The BCA is in fact exact at  $t = 0$ . See eqs. (2)-(9).
- <sup>61</sup> J. R. Dorfman and E. G. D. Cohen, *Phys. Rev. A* **12**, 292 (1975).
- <sup>62</sup> H. Gould and G. F. Mazenko, *Phys. Rev. Lett.* **35**, 1455 (1975).
- <sup>63</sup> H. Gould and G. F. Mazenko, *Phys. Rev. A* **15**, 1274 (1977).
- <sup>64</sup> D. B. Boercker, *Phys. Rev. A* **23**, 1969 (1981).
- <sup>65</sup> D. B. Boercker, F. J. Rogers, and H. E. DeWitt, *Phys. Rev. A* **25**, 1623 (1982).